The Journal of Experimental Biology 209, 965-977
Published by The Company of Biologists 2006
doi:10.1242/jeb.02066

Syringeal muscles fit the trill in ring doves (*Streptopelia risoria* L.)

C. P. H. Elemans[1,2,*], I. L. Y. Spierts[1], M. Hendriks[1], H. Schipper[1], U. K. Müller[1] and J. L. van Leeuwen[1]

[1]*Experimental Zoology Group, Wageningen University, Marijkeweg 40, 6709 PG, Wageningen, The Netherlands and* [2]*Department of Biology, University of Utah, 257S 1400E, UT 84112, Salt Lake City, USA*

*Author for correspondence (e-mail: elemans@biology.utah.edu)

Accepted 27 December 2005

Summary

In contrast to human phonation, the virtuoso vocalizations of most birds are modulated at the level of the sound generator, the syrinx. We address the hypothesis that syringeal muscles are physiologically capable of controlling the sound-generating syringeal membranes in the ring dove (*Streptopelia risoria*) syrinx. We establish the role of the tracheolateralis muscle and propose a new function for the sternotrachealis muscle. The tracheolateralis and sternotrachealis muscles have an antagonistic mechanical effect on the syringeal aperture. Here, we show that both syringeal muscles can dynamically control the full syringeal aperture. The tracheolateralis muscle is thought to directly alter position and tension of the vibrating syringeal membranes that determine the gating and the frequency of sound elements. Our measurements of the muscle's contractile properties, combined with existing electromyographic and endoscopic evidence, establish its modulating role during the dove's trill. The muscle delivers the highest power output at cycle frequencies that closely match the repetition rates of the fastest sound elements in the coo. We show that the two syringeal muscles share nearly identical contraction characteristics, and that sternotrachealis activity does not clearly modulate during the rapid trill. We propose that the sternotrachealis muscle acts as a damper that stabilizes longitudinal movements of the sound-generating system induced by tracheolateralis muscle contraction. The extreme performance of both syringeal muscles implies that they play an important role in fine-tuning membrane position and tension, which determines the quality of the sound for a conspecific mate.

Key words: biomechanics, bioacoustics, muscular control, vocal control, ring dove, *Streptopelia risoria*.

Introduction

The singing behavior of birds is an important model system for the study of motor control of learned behavior (Brainard and Doupe, 2002; Chiel and Beer, 1997; Margoliash, 2003; Liu et al., 2004), demonstrating many parallels with speech acquisition in humans (Doupe and Kuhl, 1999). Hence, many studies have focussed on the neural pathways for perception and control of song on the one hand (e.g. Bolhuis et al., 2000; Kao et al., 2005; Reiner et al., 2004; Solis et al., 2000) and behavioural aspects of the produced sound (Bradbury and Vehrencamp, 1998) on the other. To understand how a brain stimulus translates into sound, we need to know the mechanical behaviour of the interface between the two, which is provided by the muscles that control the avian vocal apparatus, the syrinx.

Both songbirds and non-songbirds generate sound by flow-induced vibrations of the labia and syringeal membranes, respectively (Fee et al., 1998; Fletcher, 1988; Gardner et al., 2001; Laje et al., 2002; Mindlin et al., 2003; Mindlin and Laje, 2005). Birds possess several syringeal muscle pairs (King, 1989). The functions of individual syringeal muscles that have been studied were derived either from correlating electromyographic (EMG) recordings with parameters such as respiratory pressure, syringeal airflow and sound characteristics (e.g. Brackenbury, 1979; Gaunt et al., 1982; Goller and Suthers, 1996a; Goller and Suthers, 1996b; Suthers et al., 1999; Vicario, 1991) or from direct endoscopic observations of the mechanical action of the muscles when stimulated *in situ* (Goller and Larsen, 1997a; Goller and Larsen, 1997b; Larsen and Goller, 1999; Larsen and Goller, 2002). These studies established that songbirds use six or more pairs of intrinsic syringeal muscles to control the position and tension of bilateral external or internal labia (Goller and Larsen, 2002; Goller and Suthers, 1995; Suthers, 1990). Pigeons, however, have only two pairs of antagonistic muscles that control position and tension of their syringeal membranes (Goller and Larsen, 1997a).

While these endoscopic and EMG studies convincingly demonstrated that muscle contractions affect the labial configuration, we still do not know how the muscles effect control because the mechanical action of a muscle cannot be inferred reliably from EMG activity alone. Furthermore, we do

not know the quantitative effects of muscular contraction on syringeal reconfiguration. From an extensive body of literature on muscle physiology, we know that the force and power output of a muscle strongly depend on its contractile properties, architecture, activation level and strain regime (e.g. Askew and Marsh, 2001; Dickinson et al., 2000; Josephson, 1985; Rome et al., 1988). These factors are all essential and largely unknown for syringeal muscles.

In this study, we test the hypothesis that syringeal muscles are physiologically able to control the syringeal aperture by mapping the contractile performance of syringeal muscles, in particular the link between strain, frequency and power during cyclic contractions. We chose ring doves (*Streptopelia risoria*) because their relatively simple syrinx contains only two muscle pairs to control sound generation at the syringeal membranes (Fig. 1). The ring dove's most common vocalization, the perch coo, consists of two syllables, *S1* and *S2*, separated by a pause *p*. The second syllable *S2* starts with a trill (*tr*) with a repetition rate of about 20 Hz. Rapid frequency modulations occur during the trill. By analogy to the pigeon (*Columba livia*), vibrations of the paired lateral tympaniform membranes (LTM) most likely produce sound (Goller and Larsen, 1997b; Larsen and Goller, 1999). The sound is filtered by the upper vocal tract (Beckers et al., 2003b; Fletcher et al., 2005; Riede et al., 2004). Both the syringeal membranes' position and tension determine the gating and the frequency of the sound (Fee et al., 1998; Fletcher, 1988; Gardner et al., 2001; Laje et al., 2002; Mindlin et al., 2003). Position and tension of the LTM are controlled by a complex interplay of forces exerted on the LTM, whose absolute magnitudes and interactions are largely unknown. Firstly, force is exerted on the LTM by the bronchial pressure. The bronchial–tracheal pressure gradient induces self-sustained oscillations of the LTM, which generate the sound wave. Secondly, force is exerted by a difference between the pressure in the bronchi–trachea and the pressure in the interclavicular air sac (ICAS). This pressure difference leads to a net force on the LTM and thus an overall tension change. In ringdoves pressure in the ICAS correlates with the fundamental frequency of the phonation (Beckers et al., 2003a). Thirdly, force is exerted by two paired extrinsic muscles, the m. tracheolateralis (TL) and m. sternotrachealis (ST). The TL applies an abductive force directly on the LTM, and the ST adducts the LTM indirectly by pulling the syrinx caudad (Goller and Larsen, 1997b; Gaunt et al., 1982; Warner, 1972). The ST and TL muscles pull in parallel but opposite directions. Anatomical drawings have tended to misrepresent this fact. The syringeal aperture resulting from LTM excursion varies from 0 mm (fully closed) to 3 mm (tracheal diameter).

Of all the coo elements, the trill requires the fastest control over the LTM position and tension. The TL is the most promising candidate for modulating membrane position and tension during the trill, because (i) it inserts directly on the LTM and (ii) its EMG activity correlates with gating and frequency modulation during the trill (Elemans et al., 2004; Gaunt et al., 1982). The role of the ST has not yet been established (Goller and Larsen, 1997b). Gaunt et al. (Gaunt et al., 1982) observed

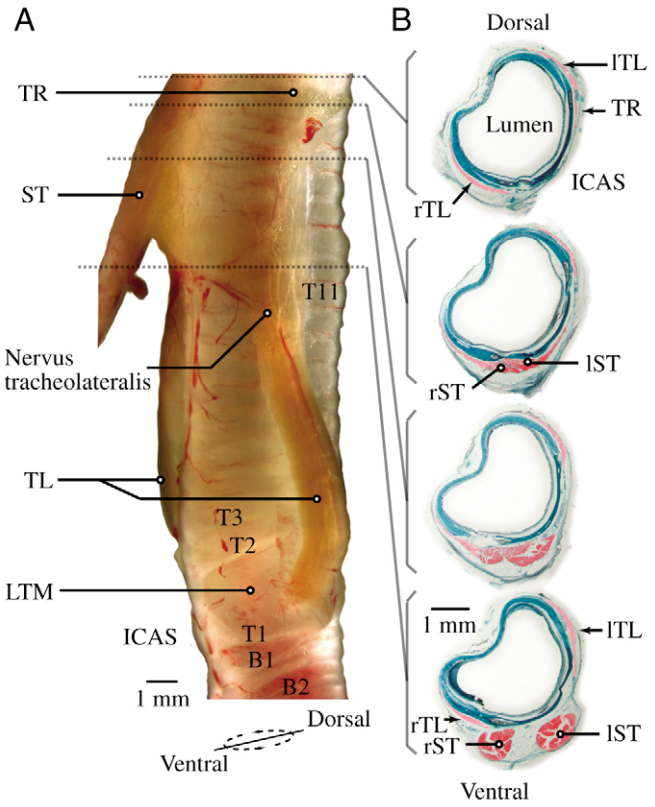

Fig. 1. Syrinx morphology. (A) Morphology of the fresh syrinx of a male ring dove. The m. tracheolateralis (TL) inserts on the lateral tympaniform membrane (LTM). Because the TL muscle fibers seemingly overlap rostrally with fibers of the m. trachealis (TR), the origin of the TL cannot be determined exactly *in vivo*. The left and right m. sternotrachealis (ST) run together in several layers of fascia from their origin around tracheal ring T17–T19. The muscle fibers of the left ST overlap the fibers of the right ST. Around T12, the two muscles split, run through the interclavicular air sac (ICAS) separately and insert bilaterally on two protuberances of the sternum (not shown). (A different version of the image in A was also provided in the supplementary information accompanying Elemans et al., 2004.) (B) Sections through the trachea and syrinx using Masson's Trichrome stain. Muscle fibers of the TL and TR can be distinguished by following the sarcolemma in subsequent sections. The ST runs in the midline of the body, because the syrinx is tilted considerably with respect to the body. B1, B2, bronchial rings; LTM, Lateral tympaniform membrane; T1–T11, tracheal rings; prefix r and l indicate right and left, respectively.

EMG modulation for the ST during the trill. Smith (Smith, 1977) claimed that cutting the ST did not affect 'normal' phonation in pigeons, but data supporting this assertion were not provided.

To gate the individual trill elements, the syringeal muscles must be able to control the syringeal aperture at high trill rates of 20 Hz, as argued above. Isometric measurements have already shown that both syringeal muscles are superfast (Elemans et al., 2004). To determine whether the muscles can indeed generate the power to be able to move the syringeal membranes in and out of the air stream, we need to extend our isometric analysis to the dynamic situation.

Materials and methods

The work loop technique was used to determine the mechanical power output of both syringeal muscles *in vitro*. The syringeal muscles were isolated from the syrinx as whole muscle preparations and subjected to an array of sinusoidal length changes, cycle frequencies and stimulation patterns. This technique is described in detail elsewhere (Askew and Marsh, 2001; Josephson, 1985).

Subjects

For the *in vitro* study, performed at Wageningen University in the Netherlands, nine adult male ring doves (*Streptopelia risoria* L., body mass M_b=156±9 g) were commercially obtained in Rotterdam, the Netherlands. Ring doves were anaesthetized with a CO_2/O_2 gas mixture and decapitated. Rectal temperature was recorded (to ±0.1°C; Lutron TM-906A, Taipei, Taiwan) while the animals were anaesthetized.

For the *in vivo* EMG study performed at the University of Utah, USA, eight adult male ring doves (M_b=152±14 g) were commercially obtained in Salt Lake City, USA.

Morphology of the syringeal muscles in ring doves

To study the exact attachment sites of the TL and ST, the syrinxes of two male adult ringdoves were sectioned and stained with Masson's Trichrome stain (Kiernan, 1990). The muscle fascia were identified in consecutive sections (Nikon Microphot-FXA, Badhoevedorp, The Netherlands) and photographed (Olympus DP50, Zoeterwoude, The Netherlands). *Toto* images of the syrinx were made with a stereomicroscope (Zeiss SV11, Sliedrecht, The Netherlands). Multiple images were combined to generate a high-resolution overview using 2D cross-correlation algorithms (AnalySIS pro, Münster, Germany).

In vivo study: EMG and sound recordings

The electromyographic (EMG) activity of musculus tracheolateralis (TL) and m. sternotrachealis (ST) were recorded in spontaneously vocalizing male ring doves. Teflon-coated copper wire electrodes (65 μm diameter) with 1 mm tips of Nickel wire (25 μm diameter) were inserted about 2 mm apart in the muscle body. Using methods similar to those described (Gaunt et al., 1982), measurements suffered from severe movement artefacts due to syrinx vibrations at 400–800 Hz (tested on three spontaneously vocalising male subjects; results not shown). Separated electrodes provided a signal from several motor units at low impedance and a better signal-to-noise ratio, and minimised movement artefacts. The electrodes were glued to the fascia with cyanoacrylate tissue adhesive, routed out of the interclavicular airsac and led subcutaneously to a backpack, as described in detail elsewhere (Goller and Suthers, 1996a; Goller and Suthers, 1996b). Spontaneous vocalizations started 1–2 days after surgery. The caged bird was placed in the centre of a larger box (1 m^3 volume), open at the front, with sound-insulating foam to suppress reflections. Sound was recorded at 20–30 cm from the cage using two microphones (Audiotechnica AT835b, Stow, OH, USA, and for calibrations a 1/4″ Brüel & Kjær omni-directional condenser microphone model 4939, Veenendaal, The Netherlands). Signals were filtered (Brown-Lee Precision Instruments, model 410, San Jose, CA, USA) and digitized at a sample frequency of 12.5 kHz using a 12-bit A/D converter (National Instruments PCI 6036, Kaysville, UT, USA). We obtained EMG signals from three healthy, spontaneously vocalising males. In individual D#1, both sound and EMG signals showed distinct pulses in the trill of syllable *S2*, and the quality of both signals allowed for analysis using single thresholds. In individual D#2, the sound modulations were not distinct enough and in individual D#3, the sound amplitude of the *S2* syllable was too weak after surgery to analyse individual sound pulses in the trill.

To calculate parameters of the sound and EMG signals, we constructed bins of 10 ms (125 points) sliding over the time signal with a shift of 1 ms (13 points). We calculated the root mean square (RMS) value and the fundamental frequency of every bin of the sound signal. To determine the fundamental frequency, we estimated the power spectral density using the periodogram method (Oppenheim and Schafer, 1989). Every bin was zero padded to 8192 points, resulting in a frequency resolution of 3.1 Hz. EMG signals were integrated with a time constant of 1 ms. To create binary signals, the EMG and sound signals were thresholded using a value equal to 3–4 times the standard deviation (s.d.) of a 100 ms no-activity segment. We conducted standard cross-correlations to determine the relationship between thresholded, integrated EMG and sound signals. We compared correlations using a Wilcoxon Signed Rank test (Zar, 1998). Experiments followed federal regulations and approval for animal experimentation at the University of Utah.

In vitro study

Sound recordings

Individual coos of all animals used in the *in vitro* study were recorded in a semi-anechoic chamber (Brüel & Kjær condenser microphone 4939; pre-amplifier 2670; amplifier Nexus dual channel) at Wageningen University. Signals were digitized at a sample frequency of 12 kHz using a 12-bit A/D converter (National Instruments PCI MIO 16E4) with a built-in amplifier. All analysis software was written in-house in Matlab (The Mathworks Inc., Gouda, The Netherlands). Mean trill repetition rate (TRR) was defined as the reciprocal of the time between the middle of successive trill elements, averaged over all trill elements for each coo.

Muscle performance

We dissected the syrinx and part of the trachea including TL and ST. To isolate the left TL, the syrinx was cut medially from the fusion point of the bronchi along the trachea (black dotted line in Fig. 2A). The exact origin of the TL muscle fibres could not be determined *in vivo*, because the fibres seemingly merged with fibres of the m. trachealis that run along the trachea towards the larynx. Based on observations of histological sections, the trachea was cut at the twentieth tracheal ring

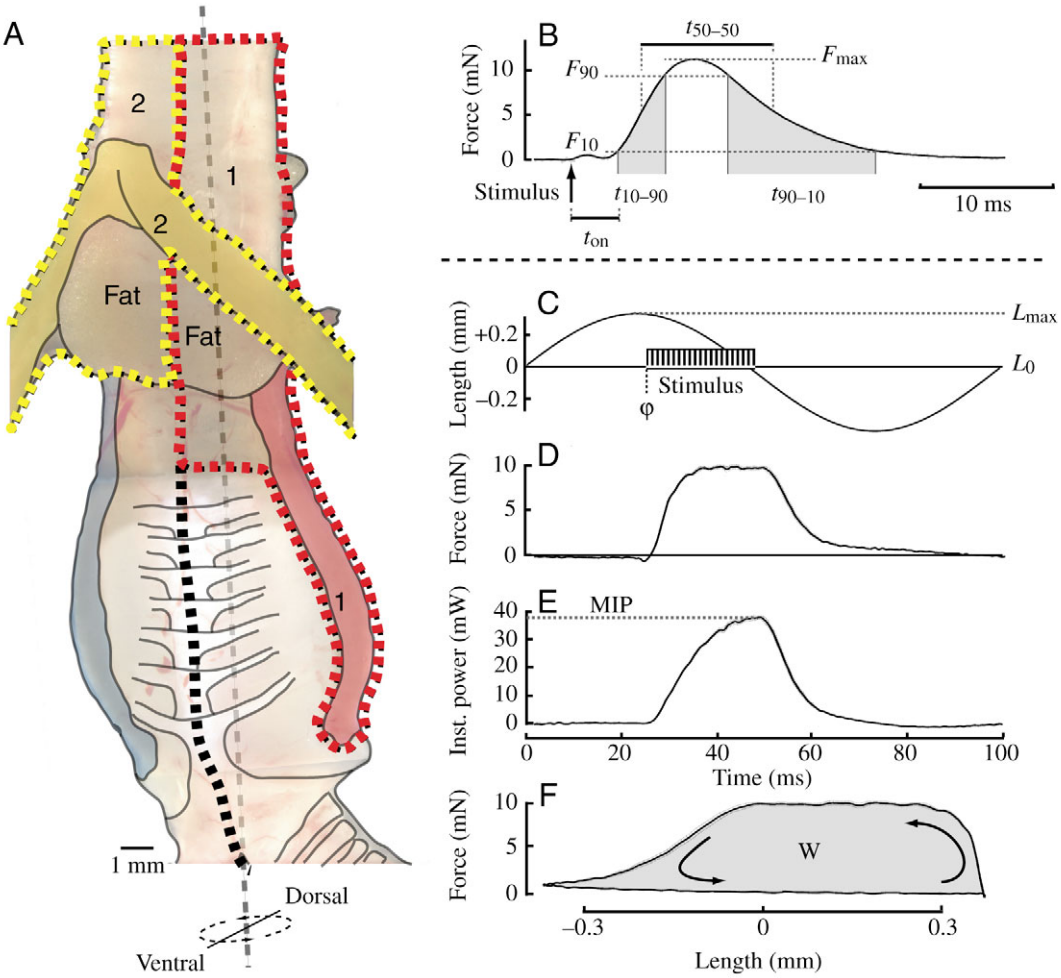

Fig. 2. Muscle preparations and measurements on muscle performance. (A) Ring dove syrinx. The dotted lines indicate dissection cuts for whole muscle preparations (1 and 2). (B) Twitch characteristics of a single-pulse muscle stimulation. Arrow indicates the onset of the stimulus. F_{10}, F_{50} and F_{90} are defined as 10%, 50% and 90% of the maximum force F_{max}. t_{on}, time between stimulus and onset of muscle contraction; $t_{10–90}$, time to ascend from F_{10} to F_{90}; $t_{90–10}$, time to descent from F_{90} to F_{10}; $t_{50–50}$, half-twitch time. (C) Muscle preparations were subjected to a sinusoidal length change with cycle frequency f and strain amplitude L_{max}. The stimulus pulse train started at phase φ (degrees) in the cycle. (D) Example of force development during cycle. (E) Instantaneous power during cycle, indicating maximum instantaneous power (MIP). (F) Workloop with shaded area W represents work. C–F are presented as mean (solid lines) ± s.d. (dotted lines) over three cycles of one series. The s.d. values are too low to be clearly discernable.

(T20) to avoid damage to TL fibres (prep. 1 in Fig. 2A). The TL was fixed in a Petri dish covered with Sylgard gel (silicone elastomere, Dow Corning Corp. Midland, MI, USA) and carefully pared down from the insertion on the membrane to T9. Some collagenous tissue from the LTM was left attached to mount the preparation in the test set-up. TL length was measured from the insertion in the LTM to T11. The paired ST could not be separated at their insertion site around T17–T19 without the risk of severe damage. Therefore, the ST were left unseparated at their insertion with a part of the trachea attached (prep. 2 in Fig. 2A). At the origin side, small bony protuberances of the sternum were left attached (typically under 1 mm). Both muscle preparations measured about 1 mm in diameter.

The preparations were fixed on Sylgard gel in Petri dishes and submerged in oxygenated Ringer's solution for birds (Askew and Marsh, 2001). In this form, they could be stored for several hours at room temperature without the performance being affected. We began measuring muscle performance alternately with TL or ST. When needed, the preparations were quickly transferred to a small chamber with circulating Ringer's solution that was saturated with oxygen. The Ringer's temperature was maintained at 39±0.1°C, which was slightly lower than the average body temperature (41.3±0.5°C, N=9), by heating a reservoir of Ringers' solution *au bain Marie* (water bath: LKB Bromma 2219, Lehman Scientific, Wrightsville, PA, USA).

The tracheal rings of the preparations were secured to the base of the experimental chamber using insect pins. At the other end, the preparations were attached to a curved insect pin

that was glued to the arm of an ergometer transducer (Dual-mode Servo series 300b, Aurora Scientific Inc., Ontario, Canada) that measured force and displacement. The TL was attached to the ergometer by pinning the collagenous LTM on the insect pin. To connect the left ST, the small piece of still attached sternum was mounted on the insect pin of the transducer. The right ST was mounted away from the transducer arm and did not affect the measured force during contraction. The position and length of the muscle was varied using three micro-manipulators. Flexible platinum wire electrodes ran parallel along the full length on opposite sides of the muscle. Stimuli were applied with a pulse generator (TGP110, Thurlby-Thandar Instruments Ltd, Huntingdon, UK). After mounting, the preparations were left to recover for about 60 min. After the experiments, all non-contractile and dead tissue was removed from the preparation and the mass (m) of the fibres was measured (to ±0.1 mg; Mettler Toledo, Tiel, The Netherlands).

The ergometer measured force and length and was controlled using the application Muscle Work (kindly provided by Drs R. K. Josephson and J. J. Malamud) developed in Labview 6.0 (National Instruments). Signals were digitized at a sample frequency of 7.5 kHz using a 12-bit A/D converter (National Instruments PCI MIO 16E4) with a built-in amplifier. Analysis software was written in-house in Matlab 6.0 (The Mathworks Inc.).

First, a series of isometric twitches and 100 ms tetanic contractions were performed to measure the twitch dynamics and isometric stress of the preparations. We used similar parameters as previous authors (e.g. Askew and Marsh, 2001; Rome et al., 1996; Young and Rome, 2001) to characterize the twitch (Fig. 2B). Maximum isometric stress (MIS, N m^{-2}) was:

$$\mathrm{MIS} = F_{\max} / A_0 , \quad (1)$$

where $F_{\max}$ is the maximal force output and A_0 is the cross-sectional area (CSA) of the muscle preparation. The CSA was assumed constant and defined as $A_0=m/(\rho L)$, where m is the mass of the preparation, ρ is the muscle density of 1060 kg m^{-3} (Mendez and Keys, 1960) and L is the length. We tuned pulse amplitude, pulse train frequency and length for each preparation to optimize the maximal force. The rest length (L_0) was defined as the length where the maximal force was generated. These preparation-specific settings were used in the work loop experiments.

Muscles were subjected to a series of five sinusoidal strain cycles with frequency f and amplitude $L_{\max}$ about L_0 (Fig. 2C). The first and last cycle were omitted from the analysis to avoid on- and offset transients. Lagrangian strain amplitude was expressed as $\epsilon=\Delta L/L_0$, with maximal amplitude ϵ_m. A run consisted of a series with stimulation (i.e. active series), followed by a series without stimulation (i.e. passive series). The measured force, length and stimulus signals of a run were aligned in time by cross-correlation of the strain signals of the two series. To estimate the force pattern solely caused by the contractile elements in the muscles, we subtracted the aligned force signals of the passive set from those of the active set (Fig. 2D). This procedure also reduced deviation in force measurements due to inertial forces at high cycle frequencies. The instantaneous power P_{inst} was $P_{\mathrm{inst}}=F(dL/dt)$ (W). The maximal instantaneous power (MIP) was measured for each cycle and averaged to obtain the value for each run (Fig. 2E). Work per cycle was defined as the area of the work loop (Fig. 2F): $W=\oint F\cdot dL$ (J). Mean power was calculated as the product of mean net work over three cycles and cycle frequency: $\bar{P}=\bar{W}\cdot f$ (W).

We stimulated the muscle preparation at various phases in the strain cycle [φ=0, 22.5, 45, 67.5, 90, 120, 162, 198 and 260° (360° comprises a full sine wave)] with a fixed duration of one quarter (=90°) of the cycle to find optimal stimulation phase. Because initial work loops at 10 Hz and a strain of 5% showed that muscle power was highest with the stimulus onset at the maximal length during 25% of the cycle, we used these stimulation settings for all further experiments. The deactivation time is short enough to enable a slightly higher duty factor at the lowest frequencies and hence to increase work output during the shortening phase. We may therefore have made a slight underestimation of the power at the lower frequencies of the investigated range. The muscles function, however, primarily at higher frequencies. We subjected the preparations to a range of cycle frequencies (TL: 5, 10, 15, 20, 25, 30, 40 and 50 Hz; ST: 1, 2, 5, 10, 20, 30, 40 and 50 Hz) and strain amplitudes [TL: 1, 2, 5, 10 and 15% (and 20% for two preparations); ST:1, 2, 5, 10, 15, 20 and 25%]. To show consistent patterns in performance between muscles, the presented MIP and mean power ($\bar{P}$) values were normalized to the maximal value within the parameter space for each preparation.

Preparations were allowed to rest for 2 min between isometric contractions and 3 min between series of work loops. Every 30 min, a twitch contraction and a run of work loops (f=10 Hz and ϵ_m=5%) was performed to monitor changes in performance. We obtained seven TL and ST preparations in good condition. The isometric data recorded from the preparations have been reported earlier (Elemans et al., 2004). The Committee of Experimental Animal Use of Wageningen University approved all experiments.

Results

Muscle morphology

The TL muscle fibres insert in the collagenous lateral tympaniform membranes (LTM) and the muscle is slightly flattened (Fig. 1B). In one specimen, we found several fibres attaching to T2–T4, while the vast majority of the fibres inserted in the LTM. More rostrally, the cross section of the TL muscle narrows to a sickle shape. The TL attaches around tracheal ring T19–T20. Detailed inspection of serial sections showed that it is distinct from the musculus trachealis (TR). We suggest that the TL can move freely in collagenous fascia during shortening. From the insertion on the trachea around T17–T19, both ST run parallel with respect to each other and the trachea for 3–4 mm out of their total length of 14–16 mm.

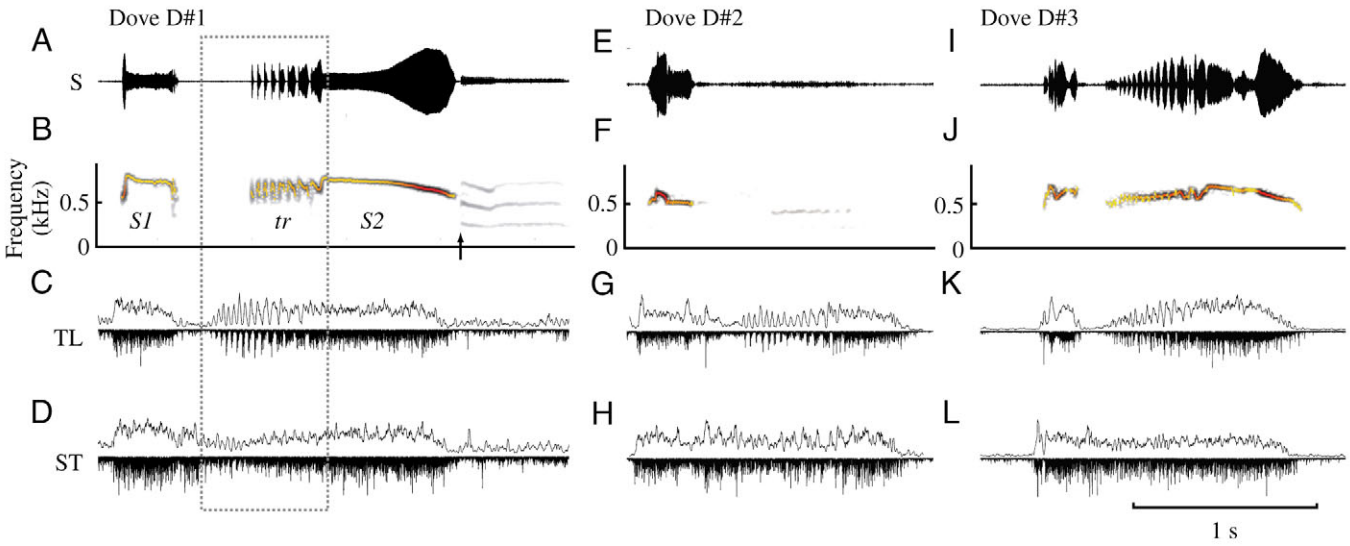

Fig. 3. Sound and muscle activity during the ring dove coo. (A,B,E,F,I,J) Typical results of (A,E,I) sound oscillograms and (B,F,J) spectrograms of the stereotyped ring dove coo, which consists of two syllables (*S1*, *S2*), followed by an inspiratory note (arrow in B) of three individuals D#1–3. Syllable *S2* starts with a trill (*tr*). The result of the fundamental frequency analysis is superimposed on the spectrogram. The colour of the trace indicates the RMS value of the corresponding bin (yellow–red; low–high). (D,C,G,H,K,L) Electromyographic recording of TL (C,G,K) and (D,H,L) ST. EMG signal: upward, rectified and integrated with time-constant of 1 ms; downward, rectified. The part of the coo in the rectangle of dove D#1 is shown enlarged in Fig. 4. The timescale is the same for all panels.

This part is suspended in the air-filled cavity of the interclavicular air sac. The ST subsequently diverge and attach to small protuberances on the ipsilateral side of the sternum close to the attachment of the pectoralis muscles. The attachment of the ST is about 1 mm to the right of the midline of the syrinx (Figs 1A, 2A). Because the syrinx is rotated axially to the left with respect to the medial body axis, the attachment of the ST on the trachea is actually in the midline of the body.

Sound characteristics

The coo of *Streptopelia risoria* consists of two syllables separated by a pause (Fig. 3A,B). The fundamental frequency of the coos produced by the animals used in the *in vitro* study ranged from 400 to 800 Hz. Syllable *S1* was 188±43 ms long and *S2* was 1117±249 ms separated by pause *p* of 296±79 ms (*N*=9). A coo lasted 1601±257 ms and was followed by an inspiratory note. These measurements agree well with reported values (Slabbekoorn and ten Cate, 1999). *S2* started with a trill that consisted of short sound elements. Repetition rate typically decreased over the trill because the duration of each consecutive element increased. The trill repetition rate (TRR) ranged from 18.8 Hz to 29.6 Hz and averaged 24.2±3.0 Hz (*N*=9). The number of trills per individual analyzed ranged from 6 to 12 elements and averaged 7.8±2.5 (*N*=9). The distinct trill elements exhibit rapid frequency modulation (see Figs 3, 4A,B).

In vivo muscle activity

Doves use both syringeal muscles simultaneously to control their song (Fig. 3). We obtained EMG signals from three individuals. From individual D#1, we obtained coos from five different bouts, of which the quality of both sound and EMG signals allowed an automated trill analysis using a single threshold (Figs 3A–D, 4). From individual D#2, we obtained

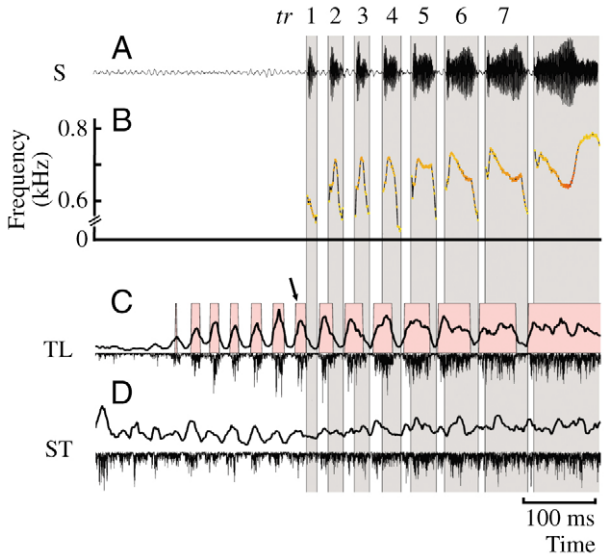

Fig. 4. Sound and muscle activity during the trill. (A) Sound oscillogram and (B) fundamental frequency of the trilled part of the coo from dove D#1. (C) TL and (D) ST EMG patterns during the trill. TL activation (red boxes) precedes the corresponding trill elements (gray boxes). Arrow shows TL burst associated with the first trill pulse (*tr* 1). ST activity shows no obvious temporal pattern. EMG signal: upward, rectified and integrated with time-constant of 1 ms; downward, rectified. This figure is modified from a previous version (Elemans et al., 2004).

coos from 15 bouts, but the second syllable *S2* decreased in sound amplitude after surgery (Fig. 3E–H). From individual D#3, we obtained coos from 11 bouts. D#3 produced trills whose elements were not separated by distinct pauses (Fig. 3I–L).

The ST is active during the entire coo for all three animals (Fig. 3D,H,L). Its activity attenuates slightly or remains constant during the silent interval between syllables (Fig. 3D,H,L). ST activity does not modulate in correspondence with individual sound elements within the trill. In contrast, TL activity modulates strongly during the trill for all three animals (Fig. 3C,G,K). TL activity correlates highly (binary signals: r=0.87±0.08; N=5) with the voiced periods of the trill for individual D#1 (Fig. 4). The correlation of TL activity with the silent periods (binary signals: r=0.55±0.14; N=5) remains strong due to the periodic nature of the signal, but it is significantly weaker (P<0.05 Wilcoxon Signed Rank test). Clearly, activating the TL muscles facilitates the vibration of the membranes and switches on the sound. Onset of TL activation precedes the onset of sound generation during the trill (compare Fig. 4B,C) by 14.8±1.1 ms (N=5). Prior to the first TL pulse associated with the first sound element in the trill (arrow in Fig. 4C), we observed pre-phonatory TL pulses that were synchronized with weak ST pulses in individual D#1 (Fig. 4). The EMG amplitude pattern of the TL in individual D#1 also correlates with fundamental frequency during the trill (r=0.88±0.07; N=5) and even the entire coo (r=0.82±0.08; N=5).

A better overview of control by the TL emerges when we look at the relationship between TL activity and fundamental frequency of the sound. Fig. 5 contains the 16 544 calculated bins of 11 coos from different bouts for individual D#3 (Fig. 5A–C) and the 9 435 calculated bins of 5 coos from different bouts for individual D#1 (Fig. 5D–F). Individual D#3 demonstrates a clear correlation between fundamental frequency and TL activity when we look at separate bins: frequency increases with TL activity (Fig. 5B). However, the separate data points are not independent measures because they are time-dependent on the oscillatory state of the LTM. If we consider the connections of each bin with adjacent bins in the time-series, we obtain the development of the signals' correlation in time (Fig. 5C,F). Fig. 5C shows that the activity of the TL does not correlate linearly with fundamental frequency throughout the coo. It is clear that in some parts of the coo, a small change in TL activity corresponds with a large change in fundamental frequency of the sound (dotted vertical line in Fig. 5C), whereas in other parts of the coo large changes in TL activity correspond with small changes in fundamental frequency of the sound (dotted horizontal lines in Fig. 5C). This pattern is also observed in individual D#1 (Fig. 5F).

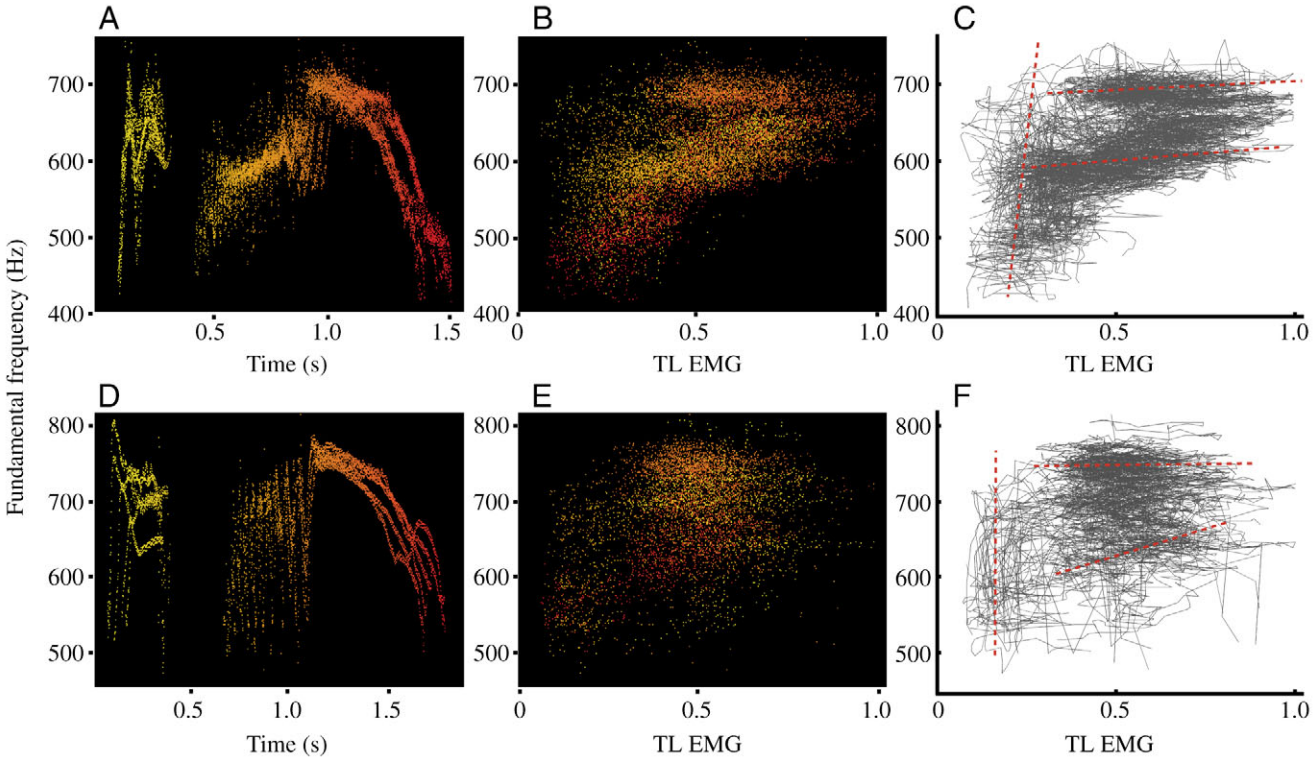

Fig. 5. Relationship between fundamental frequency and muscle activity during the coo. (A–C) Results of measurements in 16 544 calculated bins of 11 coos from different bouts for individual D#3 and (D–F) 9 435 calculated bins of 5 coos from different bouts for individual D#1. (A,D) Frequency–time relationships, linearly colour coded with time. Yellow corresponds to the start of the coo, red to the end of the coo. (B,E) Bins of integrated TL EMG activity normalised to maximal amplitude *vs* fundamental frequency of the sound with the same colour-coding as A and D, respectively. (C,F) The corresponding bin connections in time of the same bins in B and E, respectively. The dotted lines in C and F indicate regions where the relationship between TL activity and fundamental frequency of the sound differs.

Table 1. *Overview of the isometric twitch kinetics of ring dove syringeal muscles*

	Twitch characteristics (ms)				Stimulus		Maximal isometric stress (MIS)			
							Twitch contraction (kN m^{-2})		Tetanic contraction (kN m^{-2})	
	t_{on}	$t_{10–90}$	$t_{50–50}$	$t_{90–10}$	Pulse width (μs)	Pulse train frequency (Hz)	Max.	Mean	Max.	Mean
TL	3.2±0.4	3.5±0.4	9.2±0.8	10.6±1.7	214±107	250±29	18.3	8.0±4.8	32.8	18.1±7.2
ST	3.2±1.4	4.7±1.2	10.3±1.7	10.4±2.2	186±107	250±72	48.9	20.6±15.7	107.3	48.5±34.7

Mean values are ± s.d. (N=7).

See Fig. 2B for an explanation of twitch characteristics. The $t_{50–50}$, $t_{10–90}$, $t_{90–10}$ and twitch MIS values have been reported previously (Elemans et al., 2004).

In vitro muscle performance

Isometric results of the muscle preparations are listed in Table 1. Under isometric conditions, both the TL and the ST demonstrated benchmark values for superfast muscles, as reported earlier (Elemans et al., 2004). The rest lengths of TL (N=7) and ST (N=7) were 7.56±0.38 mm and 14.60±0.73 mm, respectively. The masses of the muscles were 5.4±0.8 mg and 5.7±1.4 mg, respectively. One of the ST preparations showed 50% performance decline during work loop experiments and was used only for initial isometric measurements. Under dynamic sinusoidal strain, the preparations showed the highest power output when stimulated at maximal length (φ=90° of the strain cycle) at 10 Hz (Fig. 6).

Both TL and ST generated positive power over a broad range of cycle frequencies and strains (Fig. 7). TL produced maximum mean power at 20 Hz and a strain of 10% (7.15±4.04 W kg^{-1}, normalized: 0.964±0.072, N=7). Power was not very sensitive to strain in the investigated range. TL reached maximum instantaneous power (MIP) (Fig. 7B) at 15 Hz and a strain of 20% (58.48±14.32 W kg^{-1}, normalized: 0.996±0.006, N=2). At the maximum mean power output for TL (at 20 Hz and a strain of 10%) the absolute and normalized maximum instantaneous powers were 31.00±16.86 W kg^{-1} and 0.864±0.12 (N=7), respectively. Out of seven preparations, five showed a similar pattern of maximum instantaneous power, i.e. the maximum at 20 Hz at a strain of 10%.

Mean power for ST (Fig. 7C) was highest at 20 Hz and a strain of 5% (11.62±8.85 W kg^{-1}, normalized: 0.792±0.394, N=6). The maximum instantaneous power of ST also peaked at 20 Hz and a strain of 5% (49.61±39.23 W kg^{-1}, normalized: 0.778±0.387, N=6).

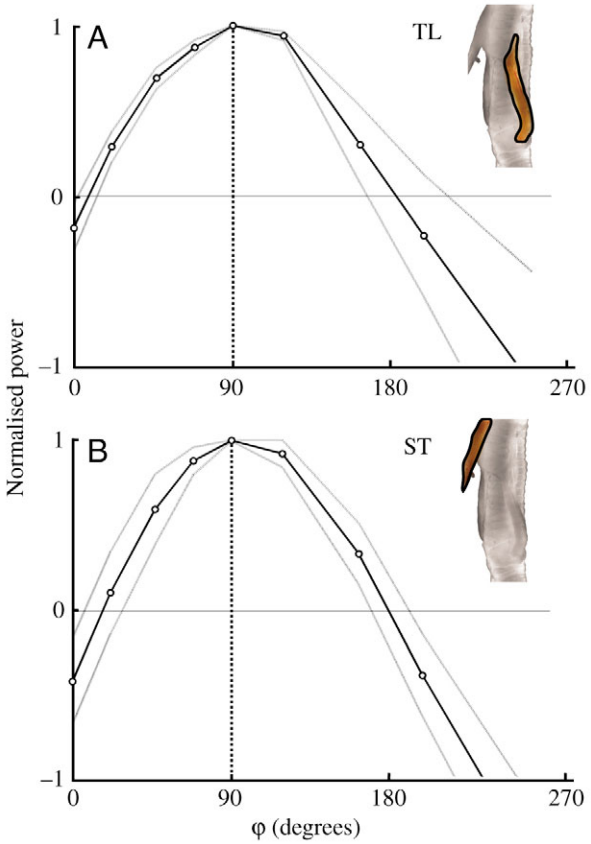

Fig. 6. Muscle performance. Muscles were stimulated at different phases (φ) in the sinusoidal shortening–lengthening cycle. Normalized power as a function of stimulation at different phases (φ) for (A) TL and (B) ST. Lines represent means ± s.d. (N=7). Cycle frequency is 10 Hz; strain, 5%. The duty factor is 25% of the strain cycle.

Biomechanical effects of the syringeal muscles

To control the physically most demanding vocal element of the dove's coo, the trill, the syringeal muscles must be able to open and close the syringeal aperture at the trill repetition rate of 24 Hz. Both the TL and ST lengths affect syringeal aperture, because contraction of either TL or ST results in a lateral excursion of the LTM (Goller and Larsen, 1997a). The syringeal aperture can be varied maximally from 0 mm (fully closed) to about 3 mm (tracheal diameter) *in situ*, which corresponds to a bilateral excursion of about 1.5 mm for each LTM. Our results show that the TL and ST have their highest power output and thus function optimally *in vivo* at strains of 10% and 5%, respectively. This corresponds to contraction amplitudes of 0.76±0.04 mm and 0.73±0.04 mm and peak-to-peak amplitudes of 1.52 mm and 1.46 mm for TL and ST, respectively, which are not significantly different (Students t-test; P<0.001). First, this shows that both muscles have a very similar mechanical dynamic range. Second, the optimal action

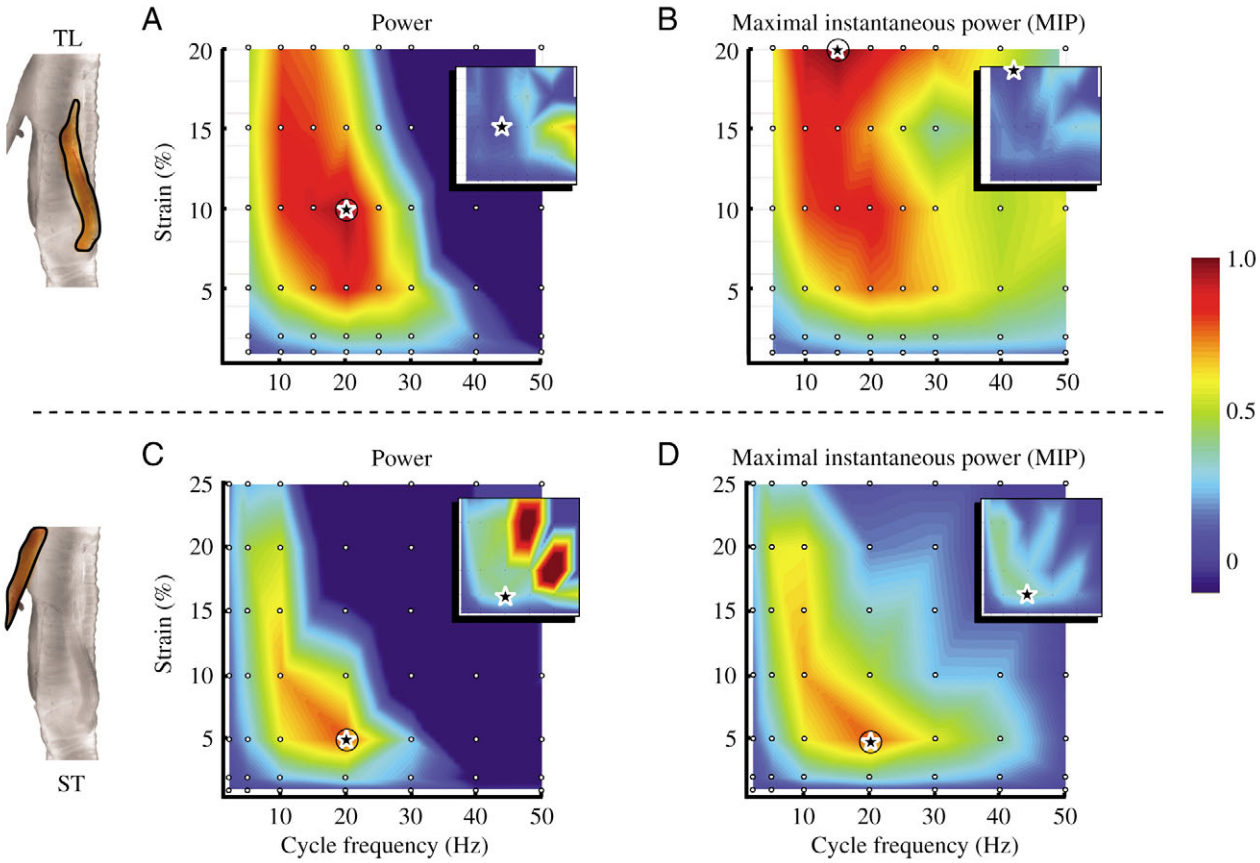

Fig. 7. Work loop results. Normalized contour plots of (A) mean power and (B) mean maximal instantaneous power (MIP) for TL preparations. (C) Mean power and (D) mean MIP for ST preparations. Insets depict the corresponding standard deviations. Values are normalized per preparation. Asterisks show local maxima. The dots show the data points measured in the strain *vs* cycle frequency parameter space.

of the syringeal muscles overlaps the *in situ* range of syringeal aperture over a range of at least 1.5 mm.

Furthermore, both muscles generate peak mean power at 20 Hz, a frequency that closely matches the mean trill repetition rate of 24.2±3.0 Hz (*N*=9). However, we used cycle frequency settings with, respectively, 5 and 10 Hz resolution, and therefore cannot determine the optimum cycle frequency of the syringeal muscles with the same precision as the trill repetition rate.

Discussion

Muscle function

We provide direct evidence that syringeal muscles are physiologically capable of the alleged muscular control of avian vocal virtuosity. The fastest song element, the trill, demands that the membranes be moved in and out of the lumen at a frequency of 24 Hz. We have shown that the m. tracheolateralis (TL) generates positive power at strains large enough to move the syringeal membranes in and out of the lumen at contraction frequencies that match the trill repetition rate. Its power output peaks at 20 Hz and remains above 65% of the maximum power at contraction frequencies between 10 and 25 Hz. The TL's insertion points – on the trachea and on the syringeal membranes – make it an effective muscle to power the cyclic movement of the syringeal membranes in and out of the lumen.

Our *in vivo* measurements show that electrical activity of the TL accompanies voiced rather than silent periods. TL activation *in vivo* precedes the onset of sound generation during the trill by 14.8±1.1 ms (*N*=5, Fig. 4). This delay between EMG and sound signal reflects the combined effect of (1) the delay between muscle activation and force development and (2) the delay between force development and significant effect on membrane position. The TL pulls the syringeal membranes apart allowing them to vibrate in the flow, which supports indirect observations that the syrinx is closed (partially) in between the trill elements (Beckers et al., 2003a). The EMG data suggest that the TL muscles exert control directly at the syringeal membranes by altering membrane position, which in turn should alter membrane tension. The proposed control mode implies that membrane position determines gating, and membrane tension determines pitch. To conclude, its anatomy, EMG activity and contractile properties all support the hypothesis that the TL moves the membranes to gait individual trill elements.

The role of the m. sternotrachealis (ST) in controlling sound generation has been unclear (Goller and Larsen, 1997a; Smith,

1977). Phonation was still possible with completely severed STs in several species of songbirds and non-songbirds (Smith, 1977). Also gas-induced phonation in anesthetised pigeons resulted in phonation (Goller and Larsen, 1997a). Gaunt et al. (Gaunt et al., 1982) report TL and ST modulations during the trill in the ring dove. When we used similar methods as described (Gaunt et al. 1982), our EMG measurements showed strong modulation in both TL and ST activity (tested on three spontaneously vocalising male subjects, results not shown). Frequency analysis showed that both TL and ST electrodes recorded energy at the coo's sound frequency. The vibrating LTMs generate vibrations with enough energy to induce vibrations of the whole syrinx and to override the energy in the recorded EMG signal. The signal modulations were caused by movement artefacts of the electrodes and not by the electrical activity of the muscles. Separation of our electrodes by about 2 mm meant that we could avoid movement artefacts due to syringeal vibrations at sound frequencies.

The ST can act as a damper

We found that the intrinsic contractile properties of the TL and ST are nearly identical: both have similar twitch kinetics and power performance distributions as a function of cycle frequency and strain. This shows that they can function as an antagonistic muscle pair. EMG recordings indicate that the ST is active during the trill, but the EMG signal does not correlate clearly with gating of the sound elements during the trill (Figs 3D,H,L, 4D). It is possible that the TL alone controls syringeal aperture to gate individual sound elements during the trill. However, such a simple control mechanism would not require a ST muscle capable of fast modulation. These observations therefore fail to explain the specialized *in vitro* properties of the ST.

Muscles have functionally diverse roles (Dickinson et al., 2000). We propose that the ST can function as a damper that stabilizes the sound-generating system. Given that the TL contracts during the trill, its insertion on the trachea can cause it to move not only the membranes but also the trachea. Such longitudinal movement of the trachea and syrinx affects the position and tension of the membranes and can thus alter the on- and offset of sound elements. The longitudinal movement of the trachea can be stabilized by a second muscle, with one insertion point on the trachea and another outside the syrinx. If this muscle were considerably slower than the driver muscle, it would let the high-frequency components pass, which can cause unwanted oscillations of the system. Cockroaches also use two muscles to stabilise their leg joint – one muscle counteracts the oscillations driven by the other – and these two muscles share similar contractile properties (Ahn and Full, 2002). The ST contractile properties, its position in the body, the mechanical effect of its contraction on the syrinx configuration, and its activity during sound generation, all agree with the hypothesis that the ST acts as a damper that counteracts longitudinal movements of the trachea.

At the same time, the ST can bring the syrinx into a different operation regime, i.e. increased ST activity probably increases the phonation threshold. In ringdoves, the TL and ST potentially have an equally important role in fine-tuning the LTM position and tension. By stabilising the trachea, the ST might enable the TL to execute subtle changes of the membrane position and tension. Such subtle changes are known to dramatically affect the perceived sound: in humans, small changes in the vocal fold affect the relative time that the fold is open *vs* closed and hence change the perceived quality of the voice (Henrich et al., 2003). Similarly in birds, a lack of stabilisation of the trachea may have detrimental effects on the quality of sound for a conspecific mate. Hence, both muscles need to cooperate to control the complex vibration of the LTM and thus the nature of the produced sound.

Frequency control in ring doves

The fundamental frequency of the produced sound in ring doves is most likely determined by the tension in the LTM, similar to human phonation (Fletcher, 1988; Gardner et al., 2001; Laje et al., 2002; Mindlin et al., 2003). As mentioned in the Introduction, the tension in the LTM is affected by a complex interplay of forces resulting from syringeal muscle activity, pressure in the air sac system and body posture that affects the positioning of the syrinx. Elemans et al. (Elemans et al., 2004) suggested that the TL controls the position and tension of the LTM and as such controls pitch and gating during phonation in ring doves. Our analysis in Fig. 5 suggests that TL control of frequency also depends on other effectors of LTM tension. One such mechanism is generation of a pressure differential between the interclavicular air sac (ICAS) and bronchial lumen (Beckers et al., 2003a; Elemans, 2004; Fletcher, 1988). Beckers et al. (2003a) found a tight correlation between fundamental frequency and temporal patterns of interclavicular air sac pressure. Combining the observations by Beckers et al. (Beckers et al., 2003a) with our data, suggests that the TL moves the LTM from a silent to a phonatory position and in this way establishes the range within which the fundamental frequency responds to pressure changes in the interclavicular air sac. The mechanism by which interclavicular air sac pressure is differentially modulated relative to the pressure in other air sacs or bronchi is not understood (Beckers et al., 2003a; Boggs et al., 2001; Duncker, 1972). With a biomechanical model of the dove's syrinx, additional knowledge on material properties and calibrated pressure signals, it would be possible to explore the separate effects of position and tension of the LTM on the fundamental frequency of the generated sound and the phonation onset, respectively.

Syringeal muscle performance

Syringeal muscles of ring doves can be classified as superfast muscles based on isometric contraction kinetics (Elemans et al., 2004). The maximum mass-specific power of about 10 W kg^{-1} that we observe in the two syringeal muscles is very low compared with 200–400 W kg^{-1} in locomotory muscles, but in the same order of magnitude as other superfast muscles, such as the toadfish *Opsanus tau* swimbladder muscle

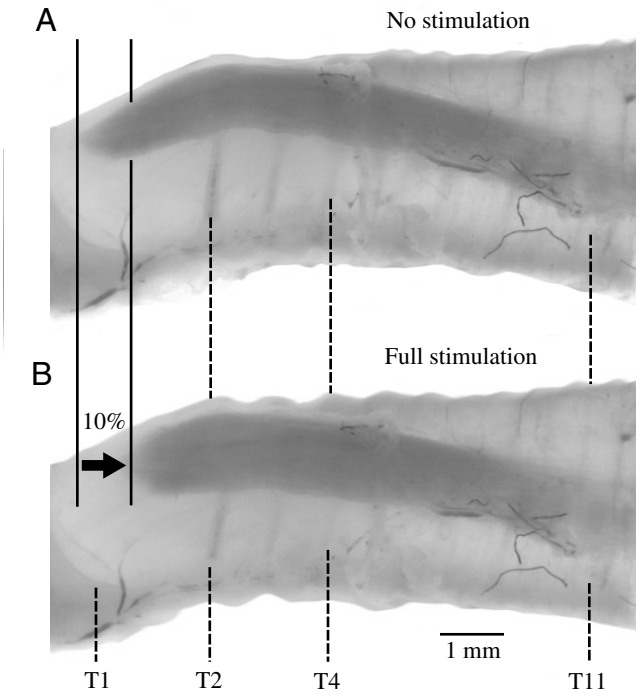

Fig. 8. *In situ* shortening of TL. *In situ* length of TL when (A) not stimulated and (B) under full stimulation. The length change is about 10%.

(Young and Rome, 2001; Fine et al., 2001; Parmentier et al., 2003; Rome et al., 1999) and western diamondback rattlesnake *Crotalus atrox* tail shaker (Rome et al., 1996). Syringeal muscles do not need to generate high power to move the LTMs.

The syringeal muscles generate maximum power at high strains compared with the swimbladder and tailshaker muscles. Because full stimulation of *in situ* preparations showed strains of 10–15% (Fig. 8), we extended the parameter space to a strain of 20%. These are high values compared with 2–4% strain at which the rattlesnake tailshaker operates (Moon et al., 2003). We did not test the performance of the syringeal muscles at very low strains, because this was not our prime interest. Therefore, we cannot estimate the maximal frequency at which positive power is still produced.

Of all the coo elements, the trill puts the highest demands on the control of sound production. The contraction speed of the syringeal muscles obviously limits the trill repetition rate. In experiments with canaries *Serinus canaria* and swamp sparrows *Melospiza georgiana*, females preferred artificial songs that consisted of notes with higher repetition rates than normal songs (Draganoiu et al., 2002; Ballentine et al., 2004). Such a selective pressure on trill repetition rate (Podos and Nowicki, 2004) or fast amplitude or frequency modulated syllables can explain the evolution of superfast syringeal muscles in ring doves, and possibly also in songbird species.

Here, we present the first data on non-isometric contraction dynamics of syringeal muscles. Yet, many essential aspects of *in vivo* use of syringeal muscles are unknown. We know neither how muscle fibres are recruited during different tasks nor how many motor units exist and how they are innervated. Furthermore, we do not know how the muscles effect control by altering muscle length *in vivo*. The TL in the ring dove could alter the position of the LTM in the airflow by short jerks using its superfast rise times or by using sinusoidal movements. To establish the optimum strain and stimulation regime for each muscle to deliver maximum power, further measurements are necessary that vary strain regime, duty cycle and activation phase. Power output might increase with longer duty cycles and asymmetric strain regimes. For example, the gray treefrog *Hyla chrysoscelis* calling muscle generated 60% more power using asymmetric strain cycles (Girghenrath and Marsh, 1999). In the case of the TL, some of the contraction is presumably taken up *in vivo* by a longitudinal compression of the trachea because both the origin and insertion sites move toward the middle of the muscle as described (Gaunt et al., 1982). Consequently, we do not know how muscle length changes of either TL or ST translate into changes of LTM position. Our data demonstrate that the optimal action of the syringeal muscles overlaps with the *in situ* range of syringeal aperture, but in an anaesthetized bird, maximal contraction of ST did not completely close the syringeal lumen (Goller and Larsen, 1997a). Measuring syringeal muscle strains during song production in freely moving birds remains a major experimental challenge.

Intrinsic muscle properties add complexity to sound production

The mechanical behaviour of the peripheral sound production system is highly non-linear and too complex to map the neural activity of motor areas in the brain directly onto the produced sound. For example, the nonlinear intrinsic material properties of the syrinx in general, and of the labia and membranes in particular, lead to sudden frequency jumps in the acoustic output (Fee, 2002; Fee et al., 1997). Furthermore, experiments and acoustical models suggest that acoustic feedback from the trachea and from beak movements (Goller et al., 2003) can play a role in introducing further nonlinearities in the relationship between labial oscillation and produced sound (Laje et al., 2001; Laje and Mindlin, 2005). The intrinsic muscle properties and the biomechanical effect of syringeal muscles on the dynamic state of the syrinx add yet another layer of nonlinearity when attempting to map the neural activity directly onto the produced sound. First, we confirmed that the force and power output of syringeal muscles are intrinsically related to their strain regime in a non-linear fashion, which is the case for any other vertebrate muscle (e.g. Woledge et al., 1985). Other current gaps in our knowledge of syringeal muscles, such as architecture at the ultra-structure level, *in vivo* activation levels, muscle fibre differentiation and recruitment, will further add to this nonlinear relationship between neural activity and force output. Second, because most biological tissues have highly nonlinear elastic properties (e.g. Vincent, 1992), small mechanical perturbations induced by the syringeal muscles alter the position and tension in vibratory tissues nonlinearly. Such small tension changes in oscillating

tissues can cause bifurcations in their nonlinear vibratory behaviour, such as the commonly observed periodic doublings in mammalian and avian phonations (Fee et al., 1998; Fee, 2002; Fitch et al., 2002; Herzel et al., 1995). In the light of the complex mechanical behaviour of the syrinx, it is more profitable to focus on the biomechanical control parameters of sound production than to attempt to correlate neural processing parameters with vocal output (Suthers and Margoliash, 2002). Therefore, we need a solid understanding of the mechanics of the sound producing system. Syringeal muscles and respiratory muscles are the motors that control the virtuosity of birds' vocalizations. Understanding their mechanical performance *in vivo* is essential to understand vocal performance and plasticity. Therefore, we ultimately need to integrate dynamical models for muscle performance into future mathematical models of sound production.

List of abbreviations

CSA	cross-sectional area
EMG	electromyograph
ICAS	interclavicular air sac
LTM	lateral tympaniform membrane
MIP	maximal instantaneous power
MIS	maximal isometric stress
RMS	root mean square
ST	musculus sternotrachealis
TL	musculus tracheolateralis
TRR	trill repetition rate

The authors thank Mees Muller and Bert Otten for interesting discussion, Otto Berg, Franz Goller and Ole Næsbye Larsen for their critical comments on earlier versions of the manuscript, and two anonymous referees for critical comments and valuable amendments on the manuscript. The investigations were supported by the Research Council for Earth and Life Sciences (A.L.W.) with financial aid from the Netherlands Organisation for Scientific Research (N.W.O.).

References

Ahn, A. N. and Full, R. J. (2002). A motor and a brake: two leg extensor muscles acting at the same joint manage energy differently in a running insect. *J. Exp. Biol.* **205**, 379-389.

Askew, G. and Marsh, R. L. (2001). The mechanical power output of the pectoralis muscle of blue-breasted quail (*Coturnix chinensis*): the *in vivo* length cycle and its implications for muscle performance. *J. Exp. Biol.* **204**, 3587-3600.

Ballentine, B., Hyman, J. and Nowicki, S. (2004). Vocal performance influences female response to male bird song: an experimental test. *Behav. Ecol.* **15**, 163-168.

Beckers, G. J. L., Suthers, R. A. and ten Cate, C. (2003a). Mechanisms of frequency and amplitude modulation in ring dove song. *J. Exp. Biol.* **206**, 1833-1843.

Beckers, G. J. L., Suthers, R. A. and ten Cate, C. (2003b). Pure-tone birdsong by resonance filtering of harmonic overtones. *Proc. Natl. Acad. Sci. USA* **100**, 7372-7376.

Boggs, D. F., Baudinette, R. V., Frappell, P. B. and Butler, P. J. (2001). The influence of locomotion on air-sac pressure in little penguins. *J. Exp. Biol.* **204**, 3581-3586.

Bolhuis, J. J., Zijlstra, G. G. O., Den Boer-Visser, A. M. and Van Der Zee, E. A. (2000). Localized neuronal activation in the zebra finch brain is related to the strength of song learning. *Proc. Natl. Acad. Sci. USA* **97**, 2282-2285.

Brackenbury, J. H. (1979). Aeroacoustics of the voal organs of birds. *J. Theor. Biol*. **81**, 341-349.

Bradbury, J. W. and Vehrencamp, S. L. (1998). *Principles of Animal Communication.* Canada: Sinauer Associates.

Brainard, M. S. and Doupe, A. J. (2002). Auditory feedback in learning and maintenance of behaviour. *Nature* **417**, 351-358.

Chiel, H. J. and Beer, R. D. (1997). The brain has a body: Adaptive behavior emerges from interactions of nervous system, body, and environment. *Trends Neurosci.* **20**, 553-557.

Dickinson, M. H., Farley, C. T., Full, R. J., Koehl, M. A. R., Kram, R. and Lehman, S. (2000). How animals move: an integrative view. *Science* **288**, 1001-1106.

Doupe, A. J. and Kuhl, P. K. (1999). Birdsong and human speech: common themes and mechanisms. *Annu. Rev. Neurosci.* **22**, 567-631.

Draganoiu, T. I., Nagle, L. and Kreutzer, M. (2002). Directional female preference for an exaggerated mail trait in canary (*Serinus canaria*) song. *Proc. R. Soc. Lond. B* **269**, 2525-2531.

Duncker, H. R. (1972). Structure of the avian lungs. *Resp. Physiol.* **14**, 44-63.

Elemans, C. P. H. (2004). How do birds sing? Sound analysis – mechanical modelling – muscular control. PhD thesis, Wageningen University, The Netherlands.

Elemans, C. P. H., Spierts, I. L. Y., Muller, U. K., van Leeuwen, J. L. and Goller, F. (2004). Superfast muscles control dove's trill. *Nature* **431**, 146.

Fee, M. S. (2002). Measurement of the linear and nonlinear mechanical properties of the oscine syrinx: implications for function. *J. Comp. Physiol. A* **188**, 829-839.

Fee, M. S., Shraiman, B., Pesaran, B. and Mitra, P. P. (1998). The role of nonlinear dynamics of the syrinx in the vocalisations of a songbird. *Nature* **395**, 67-71.

Fine, M. L., Malloy, K. L., King, C. B., Mitchell, S. L. and Cameron, T. M. (2001). Movement and sound generation by the toadfish swimbladder. *J. Comp. Physiol. A* **187**, 371-379.

Fitch, W. T., Neubauer, J. and Herzel, H. (2001). Calls out of chaos: the adaptive significance of nonlinear phenomena in mammalian vocal production. *Anim. Behav.* **63**, 407-418.

Fletcher, N. H. (1988). Bird song – a quantitative acoustic model. *J. Theor. Biol.* **135**, 455-481.

Fletcher, N. H., Riede, T., Beckers, G. J. L. and Suthers, R. A. (2005). Vocal tract filtering and the 'coo' of doves. *J. Acoust. Soc. Am.* **116**, 3750-3756.

Gardner, T., Cecchi, G., Magnasco, M., Laje, R. and Mindlin, G. B. (2001). Simple motor gestures for birdsongs. *Phys. Rev. Lett*. **87**, 208101-208105.

Gaunt, A. S., Gaunt, S. L. L. and Casey, R. M. (1982). Syringeal mechanisms reassessed: evidence from *Streptopelia*. *Auk* **99**, 474-494.

Girghenrath, M. and Marsh, R. L. (1999). Power of sound producing muscles in the gray tree frogs *Hyla versicolor* and *Hyla chrysoscelis*. *J. Exp. Biol.* **202**, 3225-3237.

Goller, F. and Suthers, R. A. (1995). Implications for lateralisation of bird sound from unilateral gating of ilateral motor patterns. *Nature* **373**, 63-66.

Goller, F. and Suthers, R. A. (1996a). Role of syringeal muscles in gating airflow and sound production in singing brown thrashers. *J. Neurophysiol*. **75**, 867-876.

Goller, F. and Suthers, R. A. (1996b). Role of syringeal muscles in controlling the phonology of bird song. *J. Neurophysiol*. **76**, 287-300.

Goller, F. and Larsen, O. N. (1997a). *In situ* biomechanics of the syrinx and sound generation in pigeons. *J. Exp. Biol.* **200**, 2165-2176.

Goller, F. and Larsen, O. N. (1997b). A new mechanism of sound generation in songbirds. *Proc. Natl. Acad. Sci. USA* **94**, 14787-14791.

Goller, F. and Larsen, O. N. (2002). New perspectives on mechanisms of sound generation on songbirds. *J. Comp. Physiol. A* **188**, 841-850.

Goller, F., Mallinckrodt, M. J. and Torti, S. D. (2003). Beak gape dynamics during song in the zebrafinch. *J. Neurobiol.* **59**, 289-303.

Henrich, N., Sundin, G., Ambroise, D., D'Alessandro, C., Castellengo, M. and Doval, B. (2003). Just noticeable differences of open quotient and asymmetry coefficient in singing voice. *J. Voice* **17**, 481-494.

Herzel, H., Berry, D. A., Titze, I. R. and Steinecke, I. (1995). Nonlinear dynamics of the voice: signal analysis and biomechanical modeling. *Chaos* **5**, 30-34.

Josephson, R. K. (1985). The mechanical power output from striated muscle during cyclic contraction. *J. Exp. Biol.* **114**, 493-512.

Kao, M. H., Doupe, A. J. and Brainard, M. S. (2005). Contributions of an avian basal ganglia–forebrain circuit to real-time modulation of song. *Nature* **433**, 638-643.

Kiernan, J. A. (1990). *Histological and Histochemical Methods: Theory and Practice*, 2nd edition. New York: Pergamon Press.

King, A. S. (1989). Functional anatomy of the syrinx. In *Form and Function in Birds* (ed. A. S. King and J. McLelland), pp. 105-192. New York: Academic Press.

Laje, R. and Mindlin, G. B. (2005). Modeling source-source and source-filter acoustic interaction in birdsong. *Phys. Rev. Lett. E* **72**, 036218.

Laje, R., Gardner, T. J. and Mindlin, G. B. (2001). Continuous model for vocal fold oscillations to study the effect of feedback. *Phys. Rev. Lett. E* **64**, 056201.

Laje, R., Gardner, T. J. and Mindlin, G. B. (2002). Neuromuscular control in vocalizations in birdsong: a model. *Phys. Rev. Lett. E* **65**, 051921.

Larsen, O. N. and Goller, F. (1999). Role of syringeal vibrations in birds vocalizations. *Proc. R. Soc. Lond. B* **266**, 1609-1615.

Larsen, O. N. and Goller, F. (2002). Direct observations of syringeal muscle function in songbirds and a parrot. *J. Exp. Biol.* **205**, 25-35.

Liu, W. C., Gardner, T. J. and Nottebohm, F. (2004). Juvenile zebra finches can use multiple strategies to learn the same song. *Proc. Natl. Acad. Sci. USA* **101**, 18177-18182.

Margoliash, D. (2003). Offline learning and the role of autogenous speech: new suggestions from birdsong research. *Speech Commun.* **41**, 165-178.

Méndez, J. and Keys, A. (1960). Density and composition of mammalian muscle. *Metabolism* **9**, 184-188.

Mindlin, G. B. and Laje, R. (2005). *The Physics of Birdsong*. Heidelberg: Springer.

Mindlin, G. B., Gardner, T. J., Goller, F. and Suthers, R. A. (2003). Experimental support for a model of birdsong production. *Phys. Rev. E* **68**, 041908.

Moon, B. R., Conley, K. E., Lindstedt, S. L. and Urquhart, M. R. (2003). Minimal shortening in a high-frequency muscle. *J. Exp. Biol.* **206**, 1291-1297.

Oppenheim, A. V. and Schafer, R. W. (1989). *Discrete-Time Signal Processing*. New Jersey: Prentice-Hall.

Parmentier, E., Genotte, V., Focant, B., Goffinet, G. and Vandewalle, P. (2003). Characterisation of the primary sonic muscles in *Carapus acus* (Carapidae): a multidisciplinary approach. *Proc. R. Soc. Lond. B* **270**, 2301-2308.

Podos, J. and Nowicki, S. (2004). Beaks, adaptation, and vocal evolution in Darwin's finches. *BioScience* **54**, 501-510.

Reiner, A., Perkel, D. J., Bruce, L. L., Butler, A. B., Csillag, A., Kuenzel, W., Medina, L., Paxinos, G., Shimizu, T., Striedter, G. et al. (2004). Revised nomenclature for avian telencephalon and some related brainstem nuclei. *J. Comp. Neurol.* **473**, 377-414.

Riede, T., Beckers, G. J. L., Blevins, W. and Suthers, R. A. (2004). Inflation of the esophagus and vocal tract filtering in ring doves. *J. Exp. Biol.* **207**, 4025-4036.

Rome, L. C., Funke, R. P., Alexander, R. McN., Lutz, G., Aldridge, H., Scott, F. and Freadman, M. A. (1988). Why animals have different muscle fiber types. *Nature* **355**, 824-827.

Rome, L. C., Syme, D. A., Hollingworth, S., Lindstedt, S. L. and Baylor, S. M. (1996). The whistle and the rattle: The design of sound producing muscles. *Proc. Natl. Acad. Sci. USA* **93**, 8095-8100.

Rome, L. C., Cook, C., Syme, D. A., Connaugthon, M. A., Ashley-Ross, M., Klimov, A., Tikunov, B. and Goldman, Y. E. (1999). Trading force for speed: Why superfast crossbridge kinetics leads to superlow forces. *Proc. Natl. Acad. Sci. USA* **96**, 5826-5831.

Slabbekoorn, H. and ten Cate, C. (1999). Collared dove responses to playback: Slaves to the rhythm. *Ethology* **105**, 377-391.

Smith, D. G. (1977). The role of the sternotrachealis muscles in bird song production. *Auk* **94**, 152-155.

Solis, M. M., Brainard, M. S., Hessler, N. A. and Doupe, A. J. (2000). Song selectivity and sensorimotor signals in vocal learning and production. *Proc. Natl. Acad. Sci. USA* **97**, 11836-11842.

Suthers, R. A. (1990). Contributions to birdsong from the left and right sides of the intact syrinx. *Nature* **347**, 473-477.

Suthers, R. A. and Margoliash, D. (2002). Motor control of birdsong. *Curr. Opin. Neurobiol.* **12**, 684-690.

Suthers, R. A., Goller, F. and Pytte, C. (1999). The neuromuscular control of birdsong. *Philos. Trans. R. Soc. B* **354**, 927-939.

Vicario, D. S. (1991). Contributions of syringeal muscles to respiration and vocalization in the zebra finch. *J. Neurobiol.* **22**, 63-73.

Vincent, J. (1992). *Structural Biomaterials.* New York: Halsted Press.

Warner, R. W. (1972). The syrinx in the family Columbidae. *J. Zool. Lond.* **166**, 285-390.

Woledge, R. C., Curtin, N. A. and Homsher, E. (1985). *Energetic Aspects of Muscle Contraction.* London: Academic Press.

Young, I. S. and Rome, L. C. (2001). Mutually exclusive designs: the power otput of the locomotory and sonic muscles of the oyster toadfish (*Opsanus tau*). *Proc. R. Soc. Lond. B* **268**, 1965-1070.

Zar, J. H. (1998). *Biostatistical Analysis*, 4th Int. Edn. New Jersey: Prentice Hall.